

Submitted to *The Astronomical Journal*

## Do OB Runaway Stars Have Pulsar Companions?

Colin J. Philp <sup>1</sup> and Charles R. Evans <sup>2</sup>

Department of Physics and Astronomy  
University of North Carolina, Chapel Hill, NC 27599-3255

Peter J. T. Leonard <sup>3</sup>

Department of Astronomy  
University of Maryland, College Park, MD 20742

Dale A. Frail <sup>4</sup>

National Radio Astronomy Observatory, <sup>5</sup> Socorro, NM 87801

*Subject headings:* Pulsars: General – Stars: Early-Type – Stars: Runaway Stars

### ABSTRACT

We have conducted a VLA search for radio pulsars at the positions of 44 nearby OB runaway stars. The observations involved both searching images for point sources of continuum emission and a time series analysis. Our mean flux sensitivity to pulsars slower than 50 ms was 0.2 mJy. No new pulsars were found in the survey. The size of the survey, combined with the high sensitivity of the observations, sets a significant constraint on the probability,  $f_p$ , of a runaway OB star having an observable pulsar companion. We find  $f_p \leq 6.5\%$  with 95% confidence, if the general pulsar luminosity function is applicable to OB star pulsar companions. If a pulsar beaming fraction of  $1/3$  is assumed, then we estimate that fewer than 20% of runaway OB stars have neutron star companions, unless pulsed radio emission is frequently obscured by the OB stellar wind. Our result is consistent with the dynamical (or cluster) ejection model for the formation of OB runaways. The supernova ejection model is not ruled out, but is constrained by these observations to allow only a small binary survival fraction, which may be accommodated if neutron stars acquire significant natal kicks.

---

<sup>1</sup>E-mail: tas@physics.unc.edu

<sup>2</sup>E-mail: evans@physics.unc.edu

<sup>3</sup>E-mail: pjtl@astro.umd.edu

<sup>4</sup>E-mail: dfrail@nrao.edu

<sup>5</sup>Operated by Associated Universities, Inc. under cooperative agreement with the National Science Foundation

According to Leonard, Hills and Dewey (1994), a 20% survival fraction corresponds to a 3-d kick velocity of  $420 \text{ km s}^{-1}$ . This value is in close agreement with recent revisions of the pulsar velocity distribution.

## 1. Introduction

The OB runaway stars are massive young stars that have high peculiar velocities ( $|V_p| > 30 \text{ km s}^{-1}$ ) and/or large scale heights above the Galactic plane (e.g.,  $> 100 \text{ pc}$ ). Such stars stand out since ordinary OB stars exhibit a scale height and velocity dispersion more typical of interstellar gas ( $\simeq 50 \text{ pc}$  and  $\simeq 10 \text{ km s}^{-1}$  respectively; Mihalas & Binney 1981). Their name derives from the fact that some of them appear to be “running away” from massive star forming regions (Blaauw & Morgan 1954; Blaauw 1989).

The two most frequently invoked explanations for the origin of OB runaways are the supernova ejection model (Blaauw 1961; Stone 1991) and the cluster, or dynamical, ejection model (Poveda, Ruiz & Allen 1967; Gies & Bolton 1986). In the first scenario, the more evolved of two OB stars in a binary system undergoes a supernova explosion which imparts a runaway velocity to its companion due to momentum conservation. Although the initially more massive primary star will be the first to explode, post main-sequence mass loss will tend to reverse the mass ratio and circularize the orbit. Thus, it is likely that the newly formed neutron star (NS) will remain bound to the surviving OB star, since half the system mass must be lost to unbind a circular binary. Even a “natal” kick of  $100 \text{ km s}^{-1}$  given to the NS (due to an asymmetric supernova) will leave most OB runaways with bound NS companions (Leonard & Dewey 1993). The newly-formed binary will acquire a significant orbital eccentricity,  $\epsilon'$ , and runaway velocity,  $V' = \epsilon' \times V_{1,orb}$ , where  $V_{1,orb}$  is the pre-supernova orbital velocity of the primary (Dewey & Cordes 1987). In contrast, dynamical ejection relies on close dynamical interactions (scatterings) involving OB binaries in young open clusters. The resulting three- or four-body interactions can eject stars at runaway velocities. This mechanism predicts that fewer than 10% of OB runaways will have companions of any kind, compact or otherwise (Leonard & Duncan 1988, 1990).

Studies aimed at trying to determine the origin of the OB runaways have relied on the binary fraction to distinguish between the above two mechanisms. Gies and Bolton (1986) conducted a search for time variations, indicative of orbital motion about a compact companion, in the radial velocities of 36 bright OB runaways. They also used existing X-ray observations of their candidates to search for evidence of accretion onto a NS or black hole. They found no evidence for compact companions which led them to favor dynamical ejection. Leonard & Dewey (1993) used a Monte Carlo program to simulate OB runaway production by the supernova ejection mechanism. They found that the upper envelope of runaway velocity is anti-correlated with mass of the progenitor system, fewer than 10% of O stars will have peculiar velocities greater than  $50 \text{ km s}^{-1}$ , and the majority of runaways will have NS companions. The authors conclude that the observations of OB runaways are better explained by dynamical ejection than supernova ejection.

Despite the above evidence for dynamical ejection, the recent discoveries of PSRs B1259-63 (Johnston et al. 1992) and J0045-73 (Bell et al. 1995), both companions to B-type main sequence stars, indicate that supernova ejection and NS retention do occur. These systems share much in common with the Be/X-ray binaries, a subgroup of the high mass X-ray binaries (HMXB) (Bhattacharya and van den Heuvel 1991), whose orbits have long periods and are highly eccentric. Indeed, PSRs B1259-63 and J0045-73 may be examples of the evolutionary step that just proceeds the formation of Be/X-ray systems. Additional evidence for supernova ejection comes from the kinematics of the HMXB (Brandt & Podsiadlowski 1995) and from the existence of the binary pulsars 1913+16 and 1534+12 which are thought to be an endpoint of massive binary evolution.

If supernova ejection occurs and some neutron stars remain bound to OB runaways, then a fraction,  $f_p$ , of the OB runaways will have pulsar companions. We conducted a search for pulsed and unpulsed radio emission at the positions of 44 OB runaways. Our search is sensitive to pulsars in long period, eccentric orbits, far from the potential obscuring effects of the OB stellar wind. The Gies and Bolton search would very likely have missed such objects because of the very small variation in the OB star’s velocity except for brief periods near periastron. Binary pulsars such as these may be common, but were missed by previous pulsar surveys because of selection effects (for example, PSR B1259-63 lies far out from the Galactic plane, has a relatively short pulse period, has a binary companion, and has not been detected at 400 MHz). Our candidate selection criteria and observations are discussed in section 2. In section 3, we discuss our sensitivity and results. Section 4 contains a Bayesian statistical analysis of our result and section 5 is a discussion of implications for runaway star formation and neutron star natal kicks.

## 2. Observations and Analysis

Detecting a pulsar in the presence of a massive stellar wind represents a two-fold problem. Firstly, the ionized wind can both scatter and absorb the radio beam coming from a pulsar, temporally broadening the pulses, reducing the pulsar’s luminosity, or possibly eclipsing it completely. Secondly, the wind may be a confusing source of thermal or non-thermal (shock) radio emission (Bieging et al. 1989). In an attempt to circumvent these problems, we adopted a two-part approach: imaging the field containing the OB star while simultaneously collecting a time series. These two aspects of the search are complimentary. If pulses are smeared out by scattering in the stellar wind, a pulsar may still be visible as a point source in the continuum map. We made images at both 1.4 and 5.0 GHz, anticipating being able to distinguish pulsars from wind emission by their tendency to have steep, negative spectral indices. We searched for pulsed emission at 1.4 GHz, rather than at a lower frequency, in order to minimize the effects of free-free absorption ( $\propto \nu^{-2}$ ) and temporal scattering ( $\propto \nu^{-4.4}$ ; Manchester & Taylor 1977). Previous pulsar searches conducted at lower radio frequencies might have systematically missed objects like PSR B1259-63 which was detected at 1.4 GHz but not at 400 MHz (Johnston et al. 1992).

## 2.1. Candidate Selection

Table 1 lists our OB runaway program stars along with their distances, peculiar velocities and spectral types. They were chosen from four sources: Bekenstein and Bowers (1974), Blaauw (1993), Conlon et al. (1990) and Gies and Bolton (1986). Our main selection criteria were that the OB runaway be near by and that the spectral type should be no earlier than O5. The first criterion seeks to insure that any potential pulsar companions will be near or above our detection sensitivity. For this reason, most of our program stars have distances less than 1 kpc. The second criterion attempts to minimize the adverse effects of the stellar wind. Mass flux from OB stars is a strong function of their mass and luminosity (Abbott 1982). Restricting the survey to B and late O stars reduces the chance of pulsar obscuration and wind emission. In addition to these criteria, we attempted to select OB runaways that have very high velocities and ones for which a birthplace in a star-forming region has been suggested (see Blaauw 1993).

## 2.2. Observations

Observations were made in February, 1994, using NRAO’s Very Large Array (VLA) near Socorro, NM. At the time of our observations, the VLA was in the hybrid D/A configuration, giving us a mix of very long and very short baselines. We observed two polarizations at 1.4 and 5.0 GHz with 50 MHz of bandwidth in each polarization. At 1.4 GHz, we used the VLA in the phased array mode, simultaneously collecting continuum visibility data and a time series. The analog sum signal was fed into a filter bank where each 50 MHz band was subdivided into 14 channels, each 4 MHz wide, to allow dedispersion of the data offline. The time series sample length was 2.6 ms. Each target was observed for a total of 12 minutes, yielding time series with  $2^{18}$  samples. In addition to the OB runaways, we observed four known pulsars for testing and calibration purposes (see Table 2).

## 2.3. Data Analysis

We carried out a standard Astronomical Image Processing System (AIPS) reduction of the visibility data. Our time series data analysis involved four major steps. In the first step, the time series were dedispersed for a range of dispersion measures (DM) from 0 to  $895 \text{ pc cm}^{-3}$  in steps of 15. In the second step, each dedispersed time series was Fourier transformed using an FFT algorithm, a power spectrum was computed and the spectrum was flattened and normalized by a running average. The third step was to choose the strongest pulsar candidate in the power spectrum. Using the fact that pulsars typically have many harmonics, the first half of the power spectrum was stretched and added to the original so that the power in a given frequency bin,  $n_b$ , would add to the power in bin  $2n_b$ . This “harmonic folding” was performed four times for each time series so that the power in the first harmonic adds to the 2nd, 4th, 8th and 16th harmonics.

A best frequency,  $f_{\text{best}} = f_{\text{max}}/n_{\text{fold}}$ , was chosen where  $f_{\text{max}}$  is the frequency with the highest signal to noise ratio (SNR) in any of the folded spectra and  $n_{\text{fold}}$  is the folding number (i.e., 1, 2, 4, 8 or 16). In the final step, the dedispersed time series was divided into segments of length  $f_{\text{best}}^{-1}$  and the segments were summed to produce an integrated time profile. Any profile having a pulsar-like shape was examined as a possible pulsar candidate.

The VLA suffers as a pulsar detection instrument in that, being an interferometer with 27 separate antennas, spurious periodic signals are present in the data from many different electronic sources. Consequently, narrow band interference must be removed from the power spectra before a best frequency is chosen. Several well-known interference signals were automatically removed from all FFTs (most notably the 19.2 Hz VLA data valid signal and 60 Hz commercial power, and their harmonics). Other interference was found by analyzing groups of sources simultaneously and comparing the best frequencies found by the search code. Matching frequencies found in two or more independent pointings were successively eliminated before folding the time series.

### 3. Sensitivity and Results

Our two search methods have different sensitivities. The continuum maps are limited by the thermal noise of the VLA electronics. The HTRP’s sensitivity is additionally limited by dispersive smearing of the pulse across the finite bandpass of the VLA and by scattering. However, in the absence of significant dispersion and scattering, the short duty cycles of most pulsars potentially allow pulse searches to have higher sensitivity than the VLA imaging counterpart.

With 12 minutes of data for each source at each frequency, the thermal noise limits for the VLA at 1.4 and 5.0 GHz are roughly 0.13 mJy and 0.10 mJy, respectively (Bridle 1989). In practice, our noise level was higher because of the unusual hybrid array configuration. Our average noise level at 1.4 GHz was  $\simeq 0.2$  mJy, giving a  $3\text{-}\sigma$  detection limit of 0.6 mJy.

To calculate our sensitivity to a pulsed signal (as a function of pulse period), we used Eq. (9) from Nice et al. (1995) with the appropriate values of average system noise, observing frequency, and filter bandwidth for the VLA. This “sensitivity curve” (Figure 1) is a plot of minimum detectable flux density (in mJy) versus pulse period (in ms). The sensitivity is also a function of DM. We used the galactic electron distribution model (and code) of Taylor and Cordes (1993) to calculate a DM for each observed OB runaway (see Table 1). Assuming a time domain SNR of 5 for an integrated pulse profile, a small duty cycle ( $< 2\%$ ) and a maximum of 32 harmonics, we calculate an average sensitivity of 0.2 mJy for long period pulsars ( $P \geq 50$  ms).

To confirm the above calculation, we introduced simulated pulsars with Gaussian profiles of random amplitudes and periods into one of our time series and then searched the data for pulses, without a priori knowledge of the amplitude, period, or even presence of a simulated pulsar. The sensitivity curve predicted well our ability to discover simulated pulsars. As a final check, two of the known pulsars which we observed, PSR J1804-0735 ( $P = 23$  ms) and PSR J0017+5914 ( $P$

= 101 ms), are sub-mJy sources (0.5 and 0.3 mJy respectively). Both were detected with high confidence.

Out of 44 program stars, we detected no pulsars and no non-thermal point sources. If we assume that pulsar companions to OB runaways have properties similar to young, non-recycled pulsars, then our search would have been sensitive to the vast majority of any such pulsars if they are not obscured by a massive wind from the OB star.

#### 4. Model Assumption and Statistics

A search of a given OB runaway may or may not turn up a pulsar. We denote by  $O_p$  the event of observing a pulsar and by  $\overline{O}_p$  the failure to detect a pulsar. Independently of the issue of detection, we denote by  $E_p$  the event of there being a potentially detectable pulsar associated with the OB star, where pulsar is here defined to mean the existence of a radio pulse emitting neutron star with its beam directed toward us that is sampled from a set of pulsars with some luminosity distribution  $\mathcal{L}$ . Conditional probabilities exist for observing a pulsar or not subject to the existence of a pulsar. In principle, the probability  $P(O_p|\overline{E}_p)$  might be nonzero if an unrelated field pulsar happens to lie within the VLA's beam or one of its sidelobes. In practice, the VLA beam is small and the chance of this occurring in any one pointing is small. In the analysis to follow we ignore unassociated field pulsars and set  $P(O_p|\overline{E}_p) = 0$ . Depending upon the assumed luminosity distribution  $\mathcal{L}$  of OB runaway pulsar companions, the distance to the star and the flux sensitivity, there will be some probability  $P_k(\overline{O}_p|E_p, \mathcal{L}, I_k)$  of *not* observing a pulsar even if one exists in any pointing  $k$ . Here  $I_k$  encapsulates instrumental and source properties, such as flux sensitivity and distance, that contribute to detectability.

Not every OB runaway will have a pulsar companion and we denote by  $f_p$  the fraction that do. There will then be some probability of obtaining a given observation  $\theta_k$  from a set of observations  $\{\theta\}$  given a value of  $f_p$ . For example, the probability of not observing a pulsar ( $\theta_k = \overline{O}_p$ ) in pointing  $k$  is

$$P_k(\overline{O}_p|f_p, \mathcal{L}, I_k) = f_p P_k(\overline{O}_p|E_p, \mathcal{L}, I_k) + 1 - f_p \quad (1)$$

since we may miss a weak pulsar, or there may be no pulsar to observe.

Bayes' formula can be used to obtain a probability distribution for  $f_p$ :

$$P(f_p|\{\theta\}, \mathcal{L}, \{I\}) = \frac{P(\{\theta\}|f_p, \mathcal{L}, \{I\})}{P(\{\theta\}|\mathcal{L}, \{I\})} P(f_p), \quad (2)$$

where  $P(f_p|\{\theta\}, \mathcal{L}, \{I\})$  is the probability density of  $f_p$  given a set of observations  $\{\theta\}$ , our model (assumed) luminosity distribution,  $\mathcal{L}$ , and instrumental and source factors,  $\{I\}$ . The probability of the set of observations, given  $f_p$ , is  $P(\{\theta\}|f_p, \mathcal{L}, \{I\})$  and  $P(f_p)$  denotes any prior knowledge of  $f_p$ . The probability density  $P(f_p|\{\theta\}, \mathcal{L}, \{I\})$  for  $f_p$  is normalized by the factor  $P(\{\theta\}|\mathcal{L}, \{I\})$ .

We failed to detect a pulsar in every pointing, so  $\theta_k = \overline{\mathcal{O}}_p$  for all  $k$ . Since each of our observations yielded a null result, we need to compute  $P_k(\overline{\mathcal{O}}_p|E_p, \mathcal{L}, I_k)$  using an assumed luminosity distribution and our sensitivity. As a model we assume that pulsar companions to OB runaways would mirror the properties of known, young, non-recycled pulsars. Using the recorded 1400 MHz luminosities of these pulsars and our sensitivity curve we compute the number of pulsars  $N_{\overline{\mathcal{O}}_p}(I_k)$  that would have gone undetected in our search. With this we can estimate the probability by

$$P_k(\overline{\mathcal{O}}_p|E_p, \mathcal{L}, I_k) = \frac{N_{\overline{\mathcal{O}}_p}(I_k)}{N_{1400}}, \quad (3)$$

where  $N_{1400} = 353$  is the total number of young, non-recycled pulsars with recorded flux at 1400 MHz. Figure 2 presents a sample calculation. Computed values of  $P_k(\overline{\mathcal{O}}_p|E_p, \mathcal{L}, I_k)$  are listed in Table 1. Note that, for most of our program stars,  $P_k(\overline{\mathcal{O}}_p|E_p, \mathcal{L}, I_k) = 0$ , reflecting the high sensitivity of our observations.

Since each of our observations was independent, the total probability  $P(\{\theta\}|f_p, \mathcal{L}, \{I\})$  is the product

$$P(\{\theta\}|f_p, \mathcal{L}, \{I\}) = \prod_{k=1}^N P_k(\overline{\mathcal{O}}_p|f_p, \mathcal{L}, I_k). \quad (4)$$

Assuming no prior knowledge of  $f_p$  and normalizing so that  $\int P(f_p|\{\theta\}, \mathcal{L}, \{I\})df_p = 1$ , we find that our null result bounds  $f_p$  to be

$$f_p \leq 0.0651, \quad (5)$$

with 95% confidence. Figure 3 shows a plot of  $P(f_p|\{\theta\}, \mathcal{L}, \{I\})$  versus  $f_p$ . To test our result's sensitivity to uncertainties in the low-luminosity tail of the pulsar luminosity distribution, we repeated the calculation assuming twice and half our stated sensitivity. The 95% confidence interval for  $f_p$  varied between 0.0647 and 0.0661, respectively, reflecting the fact that our survey was sensitive enough to detect the vast majority of pulsars consistent with our model luminosity function. Our result is consistent with the findings of Sayer et al. (1995) who conducted a similar search.

In order to draw conclusions about the mechanism for producing OB runaways, we must distinguish between pulsars and neutron stars. Four main factors could cause a NS not to be classified as a pulsar: the pulsar may never have turned on, the pulses may be obscured, they may be beamed away from us, they may have ceased because of old age. If we denote the fraction of neutron stars which never turn on by  $f_x$ , the fraction of pulsar companions to OB runaways which are obscured by  $f_o$ , the fraction that have fallen below the death line by  $f_d$ , and the fraction which are beamed toward us by  $f_b$ , then

$$f_p = f_{NS}f_b(1 - f_x - f_o - f_d), \quad (6)$$

where  $f_{NS}$  is the fraction of OB runaways having NS companions. It is difficult to set limits on  $f_o$ . However, PSR B1259-63 shows dispersive delays only very close to periastron passage (Johnston

et al. 1995), indicating that the relativistic pulsar wind comes into pressure balance with the stellar wind at a distance from the NS surface far enough to leave the pulsar undisturbed for most of the orbit. If the majority of pulsars in such systems have large spin-down luminosities, then  $f_o$  should be small. OB lifetimes range from a few to ten million years, comparable to the lifetime of a single, non-recycled pulsar. However, the lifetime of a supernova ejected OB runaway will likely be much shorter due to the pre-supernova stage of binary stellar evolution. Consequently, one can anticipate  $f_d \ll 1$ . The beaming fraction  $f_b$  is usually taken to be of order  $1/3$  (Lyne & Graham-Smith 1990). Setting  $f_x = f_o = f_d = 0$ , our observations constrain  $f_{NS} < 0.2$ .

## 5. Discussion: Implications for Runaway Star Formation and Natal Kicks of Neutron Stars

The lower than expected observed fraction of pulsar companions to the OB runaway stars has at least three interpretations. Firstly, supernova ejection may be the dominant process of ejecting stars from OB associations and those stars that retain NS companions are the HMXBs, combined with the Be and WR stars with NS companions, while the classical OB runaways represent merely the unbound minority of supernova-ejected systems. Secondly, supernova ejection may again be the dominant process producing runaways but the natal kicks that NSs receive at birth are larger than has been previously assumed which results in mostly single runaways. Thirdly, the majority of the OB runaways are dynamically ejected rather than supernova ejected.

It has been proposed that HMXBs are runaway stars (van Oijen 1989; Brandt & Podsiadlowski 1995), and so perhaps these combined with the Be stars with NS companions (Johnston et al. 1992; Kaspi et al. 1994; Schmidtke et al. 1995) and runaway WR stars with compact companions (Moffat, Lamontagne & Seggewiss 1982; Isserstedt, Moffat & Niemela 1983; Robert et al. 1992) provides a group large enough to account for the long sought after supernova-ejected runaways with NS companions. In this scenario, the classical OB runaways would represent the minority of runaway systems, from which the NSs have escaped. However, this is unlikely, since the classical OB runaways appear to outnumber the other three types of stars put together.

The observed lack of NS companions to the OB runaways may be due to larger than expected kicks given to NSs at birth. Indeed, the evidence for large natal kicks is growing (Frail & Kulkarni 1991; Cordes, Romani & Lundgren 1993; Lyne & Lorimer 1994; Frail, Goss & Whiteoak 1994). The pioneering Monte Carlo simulations of Dewey & Cordes (1987) suggest that a mean three-dimensional kick of  $90 \text{ km s}^{-1}$  is required to reproduce the observed velocity distribution and binary properties of the then-known pulsars. Curve E in Figure 2 of the more recent study of Leonard, Hills & Dewey (1994) shows that a one-dimensional kick dispersion of  $240 \text{ km s}^{-1}$  (a mean three-dimensional kick of  $420 \text{ km s}^{-1}$ ) is required to disrupt  $\simeq 80\%$  of runaway OB plus NS systems. This number is similar to the recent estimate of the mean pulsar velocity of  $450 \pm 90 \text{ km s}^{-1}$  found in the study of Lyne & Lorimer (1994). Thus, our result of 20% for  $f_{NS}$  is in very close agreement with recent revisions of the pulsar velocity distribution.



Alternatively, dynamical ejection could account for the majority of the OB runaway stars. It has been argued that this mechanism naturally accounts for many of the observed properties of the OB runaways (Gies & Bolton 1986; Gies 1987), including that the fastest dynamically-ejected runaways are expected to be single stars (Leonard & Duncan 1988, 1990; Leonard 1995). The fastest supernova-ejected systems may, in fact, be the HMXBs and perhaps the WRs with compact companions. The number of “normal looking” supernova-ejected runaway stars could be greatly outnumbered by those that result from dynamical ejection.

C.J.P. would like to thank NRAO-VLA for hospitality in summer 1993 and David Nice for helpful discussion about sensitivity. This research was supported by NSF grants PHY 90-57865 and PHY 93-17638, and by NASA grant NAGW 2934. C.R.E. thanks the Alfred P. Sloan Foundation for research support. P.J.T.L. is grateful to the University of Maryland for financial support. This research made use of the Simbad database, operated at CDS, Strasbourg, France.

## REFERENCES

- Abbott, D.C. 1982, ApJ, 259, 282
- Bekenstein, J.D. & Bowers, R.L. 1974, ApJ, 190, 653
- Bell, J.F., Bessel, M.S., Stappers, B.W., Bailes, M. & Kaspi, V.M. 1995, ApJ, 447, L117
- Bhattacharya, D. & van den Heuvel, E.P.J. 1991 Physics Reports, 203, 1
- Bieging, J.H., Abbott, D.C. & Churchwell, E.B. 1989, ApJ, 340, 518
- Blaauw, A., & Morgan, W.W. 1954, ApJ, 119, 625
- Blaauw, A. 1961, Bull. Astron. Inst. Netherlands, 15, 265
- Blaauw, A. 1989, Astrophysics, 29, 417
- Blaauw, A. 1993, in *Massive Stars: Their Lives in the Interstellar Medium*, eds. J.P. Cassinelli & E.B. Churchwell (ASP: San Francisco), p. 207
- Brandt, N., & Podsiadlowski, P. 1995, MNRAS, 274, 461
- Bridle, A.H. 1989, in *Synthesis Imaging in Radio Astronomy*, ed. R.A. Perley (ASP: San Francisco), p. 443
- Conlon, E.S., Dufton, P.L., Keenan, F.P., & Leonard, P.J.T. 1990, A&A, 236, 357
- Cordes, J.M., Romani, R.W., & Lundgren, S.C. 1993, Nature, 362, 133
- Dewey, R.J. & Cordes, J.M. 1987, ApJ, 321, 780
- Frail, D.A., & Kulkarni, S.R. 1991, Nature, 352, 785
- Frail, D.A., Goss, W.M. & Whiteoak, J.B.Z. 1994, ApJ, 437, 781
- Gies, D.R. & Bolton, C.T. 1986, ApJS, 61, 419
- Gies, D.R. 1987, ApJS, 64, 545
- Isserstedt, J., Moffat, A.F.J., & Niemela, V.S. 1983, A&A, 126, 183
- Johnston, S., Manchester, R.N., Lyne, A.G., Bailes, M., Kaspi, V. M., Qiao, Guojun & D’Amico, N. 1992, ApJL, 387, L37
- Johnston, S., Manchester, R.N., Lyne, A.G., D’Amico, N., Bailes, M. Gaensler, B.M. & Nicastro, L. 1995, MNRAS, in press
- Kaspi, V.M., Johnston, S., Bell, J.F., Manchester, R.N., Bailes, M., Bessell, M., Lyne, A.G., D’Amico, N. 1994, ApJ, 423, L45

- Leonard, P.J.T. & Dewey, R.J. 1993, in *Luminous High-Latitude Stars*, ASP Conference Series Vol. 45, ed. D.D. Sasselov (ASP, San Francisco), p. 239
- Leonard, P.J.T. & Duncan, M.J. 1988, *AJ*, 96, 222
- Leonard, P.J.T. & Duncan, M.J. 1990, *AJ*, 99, 608
- Leonard, P.J.T., Hills, J.G. & Dewey, R. J. 1994, *ApJ*, 423, L19
- Leonard, P.J.T. 1995, *MNRAS*, in press
- Lyne, A.G., & Graham-Smith, F. 1990, in *Pulsar Astronomy*, (Cambridge University Press: Cambridge), p. 164
- Lyne, A.G., & Lorimer, D.R. 1994, *Nature*, 369, 127
- Manchester, R.N., & Taylor, J.H. 1977, in *Pulsars*, (W.H. Freeman and Company: San Francisco), p. 140
- Mihalas, D & Binney, J. 1981, in *Galactic astronomy: Structure and kinematics (2nd ed.)* (W.H. Freeman and Co.: San Francisco), pp. 252 & 423
- Moffat, A.F.J., Lamontagne, R., & Seggewiss, W. 1982, *A&A*, 114, 135
- Nice, D.J., Fruchter, A.S. & Taylor, J.H. 1995, *ApJ*, in press
- Poveda, A., Ruiz, J., & Allen, C. 1967, *Bol. Obs. Tonantzintla y Tacubaya*, 4, 86
- Robert, C. et al. 1992, *ApJ*, 397, 277
- Sayer, R.W., Nice, D.J., Kaspi, V.M. 1995, submitted to *ApJ*
- Schmidtke, P.C., Cowley, A.P., McGrath, T.K., & Anderson, A.L. 1995, *PASP*, 107, 450
- Stone, R.C. 1991 *AJ*, 102, 333
- Taylor, J.H., & Cordes, J.M. 1993, *ApJ*, 411, 674
- Taylor, J.H., Manchester, R.N. & Lyne, A.G. 1993, *ApJS*, 88, 529
- van Oijen, J.G.J. 1989, *A&A*, 217, 115

Table 1. Observed OB Runaways

OB Runaway	Distance	$V_p$	Type	$DM_{\text{calc}}$	$P_k$	ref
72 Col	0.26	191	B2.5V	4.8	0.000	1
AGK+60°1562	0.55-0.7	40	B9III	13.1	0.000	1
BD+59 186	1.8-3.1	56	B5II	83.5	0.067	1
HD 4142	0.26	-60	B4V	4.9	0.000	4
HD 14220	0.61	-34	B2V	11.1	0.000	4
HD 16429	1.39	-24	O9.5III	25.6	0.008	4
HD 17114	0.7-0.9	63	B1V	16.7	0.000	1
HD 19374	0.36	59	B1.5V	6.6	0.000	1
HD 20218	1.0–1.4	40	B2V	25.5	0.008	1
HD 24912	0.51	58	O7.5	9.4	0.000	4
HD 29866	0.29	-3	B8IVn	5.4	0.000	4
HD 30614	1.25	26	O9.5Ia	22.1	0.000	1,2
HD 30650	0.41	34	B6V	7.6	0.000	4
HD 34078	0.52	49	O9.5V	9.7	0.000	2,4
HD 37737	2.16	25	O9.5III	56.0	0.025	4
HD 38666	0.7	123	O9.5V	12.5	0.000	1,2
HD 39478	0.85–1.2	49	B2V	22.0	0.000	1
HD 39680	2.48	29	O6V	55.5	0.039	4
HD 43112	0.65	19	B1V	12.0	0.000	4
HD 52533	1.82	9.6	O9V	33.1	0.014	4
HD 78584	0.89	111	B3	15.0	0.000	1
HD 91316	0.59	36	B1Ib	8.3	0.000	3
HD 97991	0.93	22	B2V	14.3	0.000	4
HD 125924	2.47	259	B2IV	20.6	0.014	3
HD 149363	1.11	148	B0.5V	19.2	0.000	4
HD 149757	0.17	39	O9.5	3.2	0.000	1,2
HD 157857	2.40	50	O7f	54.0	0.039	1
HD 172488	0.54	41	B0.5v	10.3	0.000	4
HD 188439	1.08	-58	B0.5IIIp	20.0	0.000	4
HD 189957	2.55	49	O9.5III	46.7	0.039	4
HD 192281	1.78	-32	O5e	33.5	0.014	4
HD 195907	0.92	-68	B1.5Ve	17.2	0.000	4
HD 201345	1.92	29	ON9V	34.7	0.014	4
HD 201910	0.54	4	B5V	10.1	0.000	4
HD 203064	0.85	20	O7.5	16.0	0.000	4

Table 1—Continued

OB Runaway	Distance	$V_p$	Type	$DM_{\text{calc}}$	$P_k$	ref
HD 210839	0.86	-54	O6Iab	16.1	0.000	1,2
HD 214080	2.40	32	B1/B2Ib	19.0	0.014	3
HD 214930	0.75	-46	B2IV	13.3	0.000	4
HD 216534	0.83	82	B3V	15.4	0.000	1
HD 219188	2.11	82	B0.5III	19.1	0.011	3
HD 220172	0.77	18	B3Vn	11.1	0.000	3
HD 248434	3.0-6.0	83	B5Ie	113.1	0.204	1
HD 276968	1.3-2.0	55	B9II	54.4	0.014	1
HD 333282	1.3	40	B7III	24.7	0.003	1

References. — (1) Bekenstein & Bowers 1974; (2) Blaauw 1993; (3) Conlon et al. 1990; (4) Gies & Bolton 1986.

Note. — Distances are in kpc.  $V_p$  are in  $\text{km s}^{-1}$ . DM values, in  $\text{pc cm}^{-3}$ , were calculated using the code of Taylor and Cordes (1993). Where a range of distances is given, the larger was used to calculate the DM.  $P_k$  refers to the probability,  $P_k(\overline{O}_p|E_p, \mathcal{L}, I_k)$ , of not observing a pulsar subject to the existence of a pulsar, the assumed luminosity distribution  $\mathcal{L}$ , and instrumental factors  $I_k$ .

Table 2. Observed Known Pulsars

Pulsar	Period	$S_{1400}$	DM
J0117+5914	101.44	0.3	48.5
J0147+5922	196.32	2.0	39.3
J1804-0735	23.10	0.5	186.4
J1833-0827	85.28	5.0	411.0

Note. — Pulse periods are in milliseconds.  $S_{1400}$  is the time average flux density, in mJy, at 1400 MHz. The measured DM values are in  $\text{pc cm}^{-3}$ . All values are from Taylor et al. (1993)

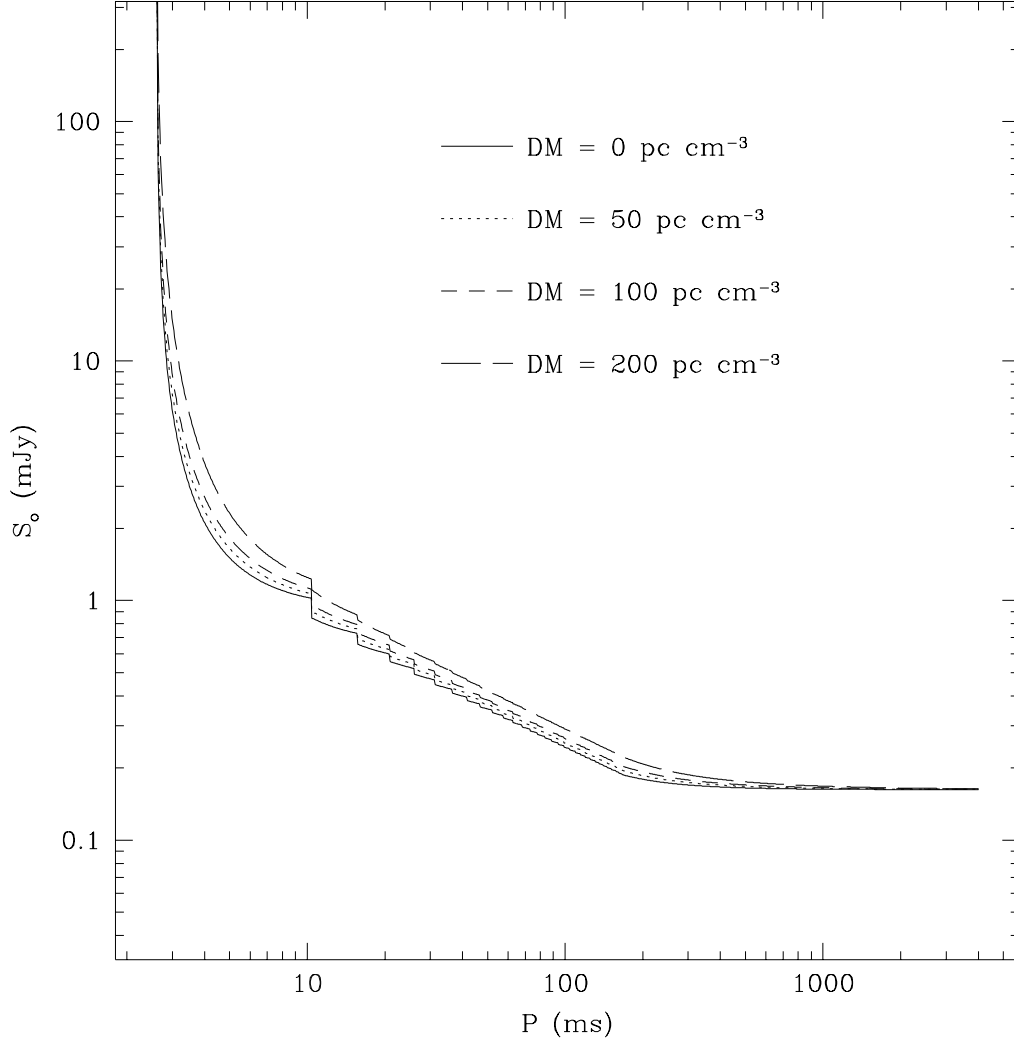


Fig. 1.— Pulsar Sensitivity. The lowest detectable flux density,  $S_o$ , is plotted as a function of pulse period. These curves were calculated using Eq. (9) from Nice et al. 1995. We assumed a signal-to-noise ratio of five (in the time domain), a small duty cycle ( $\leq 2\%$ ) and a maximum of 32 harmonics in the power spectrum.

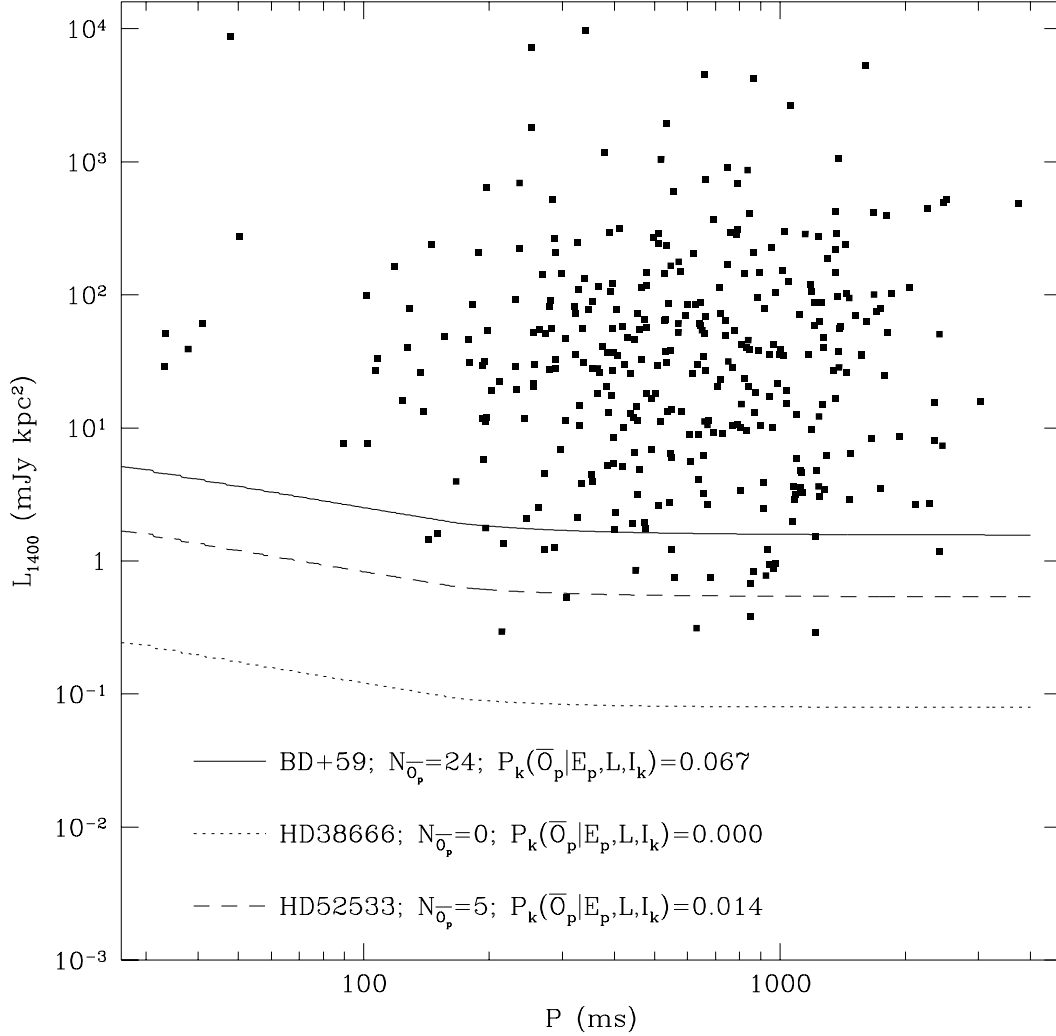


Fig. 2.— Calculation of conditional probability. The squares mark the 1400 MHz luminosities (flux density times distance squared) of the known pulsars (Taylor et al. 1993). The recycled or millisecond pulsars have been excluded because they represent a separate population. Here, the sensitivity curves (calculated for the DMs in Table 1) are scaled by the distance in order to reflect luminosity sensitivity.  $N_{\overline{O}_p}$  represents the number of known pulsars that fall below a given sensitivity curve.

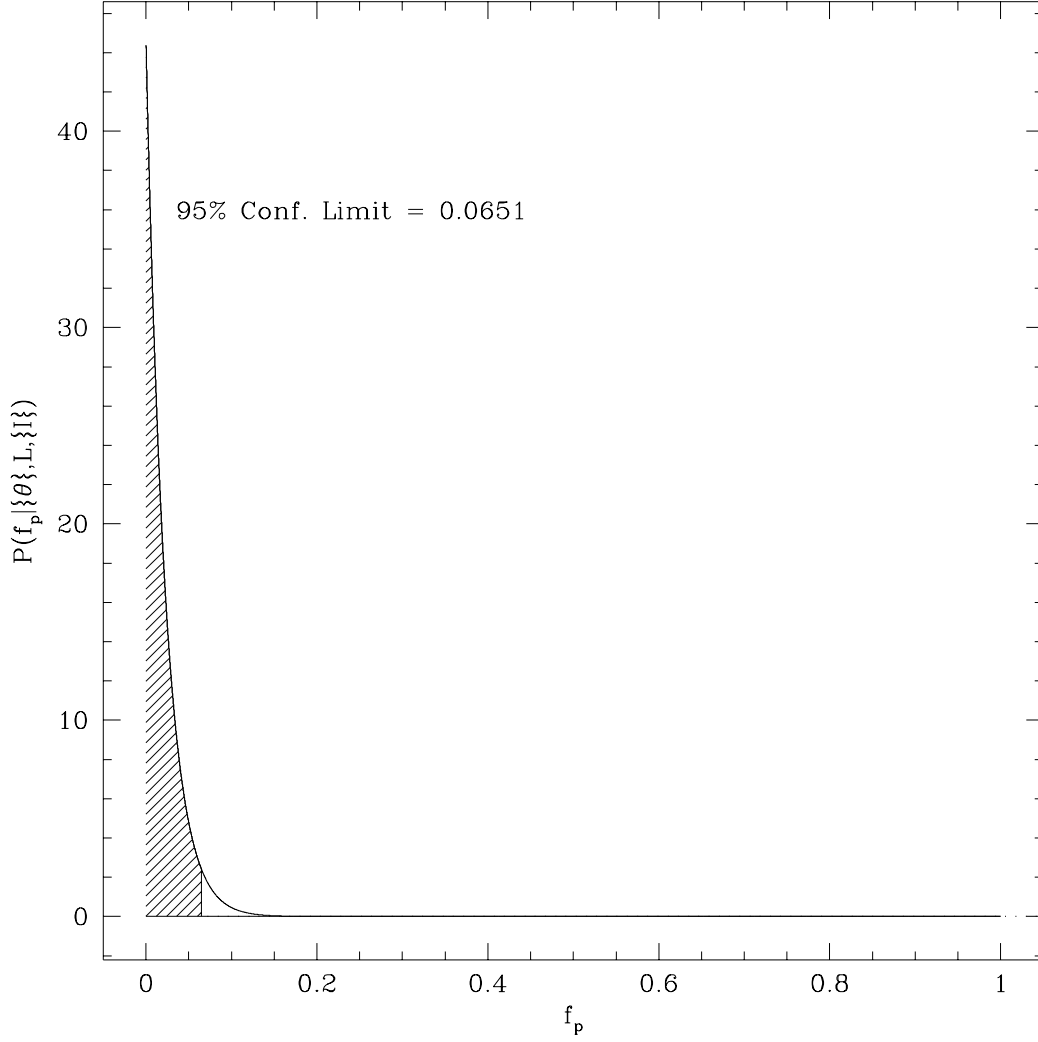


Fig. 3.— Probability Density of  $f_p$ .  $P(f_p | \{\theta\}, \mathcal{L}, \{I\})$  is normalized so that the total area under the curve equals 1.0. The 95% confidence limit is the value of  $f_p$  to the left of which the area under the curve equals 0.95 (the shaded area).